Endocannabinoid signalling selectively targets perisomatic inhibitory inputs to pyramidal neurones in juvenile mouse neocortex

Joseph Trettel, Dale A. Fortin and Eric S. Levine

Department of Pharmacology, University of Connecticut Health Center, Farmington, CT 06030, USA

Retrograde synaptic signalling has long been recognized as a fundamental feature of neural systems. However, the cellular specificity and functional consequences of fast retrograde communication are not well understood. We have focused our efforts on understanding the role that endocannabinoids play in regulating synaptic inhibition in sensory neocortex. Recent studies have implicated endocannabinoids as the retrograde signalling molecules that underlie depolarization-induced suppression of inhibition, or DSI. This short-term form of presynaptic depression is triggered by postsynaptic depolarization and is likely to play an important role in information processing. In the present study we investigated the cellular and synaptic specificity of endocannabinoid signalling in sensory cortex using whole-cell recordings from layer 2/3 pyramidal neurones (PNs) in acute brain slices. We report that GABAergic interneurones that are depolarized by muscarinic receptor stimulation provided the majority of DSI-susceptible inputs to neocortical PNs. This subclass of interneurones generated large, fast postsynaptic currents in PNs which were transiently suppressed by either postsynaptic depolarization or a brief train of action potentials. Neocortical DSI required activation of the type 1 cannabinoid receptor (CB1R) but not metabotropic glutamate or GABA receptors. Using focal drug application, we found that the DSI-susceptible afferents preferentially synapse on the perisomatic membrane of PNs, and not on the apical dendrites. Together, these results suggest that endocannabinoid-mediated DSI in the cortex can transiently and selectively depress a subclass of PN inputs. Although the physiological implications remain to be explored, this suppression of somatic inhibition may alter the excitability of principal neurones and thereby modulate cortical output.

(Received 8 December 2003; accepted after revision 21 January 2004; first published online 23 January 2004)
Corresponding author E. S. Levine: Department of Pharmacology, MC-6125, University of Connecticut Health Center, 263 Farmington Ave., Farmington, CT 06030, USA. Email: eslevine@neuron.uchc.edu

Endocannabinoids and the type-1 cannabinoid receptor (CB1R) are components of a novel neuromodulatory signalling system in the central nervous system (reviewed in Di Marzo *et al.* 1998; Freund *et al.* 2003). Endocannabinoids function, at least in part, as retrograde messengers that mediate some forms of long-term depression (LTD; Gerdeman *et al.* 2002; Marsicano *et al.* 2002; Robbe *et al.* 2002; Chevaleyre & Castillo, 2003; Sjostrom *et al.* 2003) and DSI (Kreitzer & Regehr, 2001; Ohno-Shosaku *et al.* 2001; Wilson & Nicoll, 2001). DSI, originally described in the hippocampus (Pitler & Alger, 1992, 1994) and cerebellum (Llano *et al.* 1991), is a short-term suppression of GABA release induced by postsynaptic depolarization. This type of signalling may also play a role in regulating inhibitory afferents to pyramidal neurones (PNs) in the neocortex. Diverse classes of GABAergic interneurones subdivide the membrane of PNs into distinct domains, regulating well-defined aspects of PN physiology (Kawaguchi & Kubota, 1997; Somogyi *et al.* 1998; Gupta *et al.* 2000). The selective regulation of compartmentalized inhibition via retrograde signalling may therefore be important for defining cortical output.

The cortical endocannabinoid system is well-suited to regulate specific inhibitory domains because CB1R expression is mostly restricted to the subset of GABAergic interneurones that coexpress cholecystokinin (CCK; Marsicano & Lutz, 1999). Interneurones that express CCK target the perisomatic membrane of PNs (Kubota & Kawaguchi, 1997; Kawaguchi & Kubota, 1998). In the hippocampus, CB1R is also expressed in

 DOI: 10.1113/jphysiol.2003.058198

CCK-positive basket cells (Katona *et al.* 1999; Tsou *et al.* 1999) and DSI-sensitive currents tend to be large-amplitude events with fast rise times, consistent with somatic localization (Martin *et al.* 2001; Wilson *et al.* 2001). Interestingly, cholinergic receptor activation selectively enhances hippocampal DSI partly by increasing the discharge of CCK-expressing interneurones (Martin & Alger, 1999). In the cortex, CCK-expressing interneurones are also depolarized by cholinergic agonists (Kawaguchi, 1997). Cortical endocannabinoids may preferentially modulate GABA release from the subset of CCK-expressing interneurones, thereby selectively suppressing perisomatic inhibition.

Although the cannabinoid system in the neocortex mediates many of the cognitive and behavioural effects of marijuana, there has been little study of the cortical endocannabinoid system. We have recently shown that CB1R activation suppresses GABA release from cortical interneurones (Trettel & Levine, 2002), consistent with the effects of exogenous cannabinoids on GABA release in frontal cortex *in vivo* (Ferraro *et al.* 2001). We have also shown that endocannabinoids mediate a DSI-like phenomenon of evoked inhibitory currents in neocortex (Trettel & Levine, 2003). Evoked currents, however, represent the synchronous activation of a heterogeneous population of synapses arising from diverse cell types, and the change in amplitude provides little information regarding the inputs that are suppressed. In order to understand the physiological significance of this retrograde synaptic signalling, an important first step is to identify the specific inhibitory inputs that are modulated by endocannabinoid-mediated DSI. In the present studies we recorded spontaneous inhibitory postsynaptic currents (sIPSCs) and postsynaptic potentials (sIPSPs) to characterize DSI-susceptible afferents and to determine the spatial distribution of their synaptic contacts on the postsynaptic PN membrane.

Methods

Brain slice preparation

Swiss CD-1 mice (P12-20; Charles River) were killed by exposure to a rising concentration of CO_2 followed by rapid decapitation according to procedures approved by University of Connecticut Health Center Animal Care Committee. Brains were rapidly dissected into ice-cold cutting saline that was composed of (mM): 125.0 NaCl, 2.5 KCl, 1.25 NaH_2PO_4, 25.0 $NaHCO_3$, 0.5 $CaCl_2$, 4.0 $MgCl_2$, 17.5 glucose and gassed with 95% O2–5% CO_2 (pH 7.3, 315 $\pm$ 3 mmol kg^{-1} osmolality). The tissue was then sectioned at 300 μm (DTK-1000, Dosaka) in the anatomically transverse plane. Cortical slices containing auditory and visual fields (Frisina & Walton, 2001; Paxinos & Franklin, 2001) were incubated for 30–45 min in a custom submersion-type recovery chamber that was filled with normal saline at 35°C. These granular, sensory regions were easily demarcated from surrounding cortical fields by the relative packing density of neurones and the robustness of layer 4. The normal saline, or artificial cerebrospinal fluid (ACSF), was composed of (mM): 125.0 NaCl, 2.5 KCl, 1.25 NaH_2PO_4, 25.0 $NaHCO_3$, 2.0 $CaCl_2$, 2.0 $MgCl_2$, 17.5 glucose and gassed with 95% O_2–5% CO_2 (pH 7.3, 315 $\pm$ 3 mmol kg^{-1}). After recovery, the slices were subsequently transferred to a recording chamber fixed to the stage of an upright microscope that was perfused with fresh oxygenated saline (32 $\pm$ 0.5°C) and allowed to acclimate for 5–10 min prior to recording.

Electrophysiology

Whole-cell recordings of sIPSCs and sIPSPs were made from layer 2/3 PNs. Ionotropic glutamate receptors were blocked with bath perfusion of 6,7-dinitroquinoxaline-2,3-dione (DNQX, 10 μM, Tocris, Bristol, UK) and 3-((*R*)-2 - carboxypiperazin - 4-yl)-propyl-1-phosphonic acid (CPP, 2 μM, Tocris). Individual neurones were visualized using an Olympus BX51W microscope equipped with infrared differential interference contrast optics. All neurones in our sample had the characteristic pyramidal-shaped soma with a single apical dendrite; PNs responded to depolarizing current injection with regular, frequency-adapting spikes that are typical of these neurones (e.g. McCormick *et al.* 1985; Connors & Gutnick, 1990).

Voltage clamp recordings were made with borosilicate glass micropipettes (pipette resistance (R_p) = 3–5 MΩ) filled with (mM): 120.0 CsCl, 10.0 Hepes, 1.0 EGTA, 0.1 $CaCl_2$, 1.5 $MgCl_2$, 4.0 Na_2-ATP, 0.3 Na-GTP and 5.0 QX-314 (pH 7.3, 293 $\pm$ 2 mmol kg^{-1}). Prior to use the glass pipettes were lightly heat polished. Synaptic currents were filtered at 2.9 kHz and digitized at $\geq$6 kHz using a HEKA EPC9/2 amplifier and a PCI-16 interface board (Heka Elektronic, Darmstadt, Germany). Neurones were voltage clamped at –70 mV. Upon breaking into whole-cell configuration, a brief series of voltage ramps (50 ms, 2 mV ms^{-1}) were applied to promote the activity-dependent block of Na^+ conductances by QX-314 (Sigma, Missouri, USA). Series resistance (R_s) was then compensated to 60% or greater at 10–100 μs lag. During the course of the experiments, leak currents were subtracted online (*P*/4) and the input resistance

(R_i) was monitored continuously with 5 mV hyperpolarizing voltage steps (50 ms). Neurones were rejected from analyses if: (1) R_s was >25 MΩ at the time of break-in or >10.5 MΩ after compensation, (2) R_i changed by >15% during the course of an experiment, or (3) R_i fell below 100 MΩ. For current clamp recordings, the internal pipette solution contained (mM): 130 KCl, 0.10 $CaCl_2$, 10 Hepes, 1 EGTA, 4 Na_2-ATP, 0.3 Na-GTP and 10 phosphocreatine (pH 7.3, 285 ± 2 mmol kg^{-1}). Brief trains of action potentials (20 Hz) were induced by injecting square-wave current pulses (pulse duration = 5 ms; amplitude = 1 nA). Cells were rejected from the analysis if: (1) V_m was below –60 mV, (2) R_i changed by >15% during the course of an experiment, or (3) R_i fell below 100 MΩ.

GABA and bicuculline (BIC) were focally applied to PN membranes with unpolished glass recording pipettes. GABA (100 μM, pH 3.2) was iontophoretically applied (25–50 nA ejection, –15 nA retention; ION-100, Dagan) and BIC (150 μM) was pressure applied at 5–30 kPa (Picospritzer II, Parker Hannifin). The pipette tips were placed ~15 μm from the membrane surface during iontophoresis and ~25 μm from the membrane surface during pressure ejection. Duration of drug application was 10–50 ms. All other drugs were delivered through the bath perfusion system at 2–3 ml min^{-1}. WIN55,212-2 (Sigma), AM251 (gift from Dr A. Makriyannis, University of Connecticut) and DNQX were stored in 10 mM aliquots in DMSO at –20°C. Final DMSO concentration did not exceed 0.03%.

Data analysis

Off-line analysis was carried out using PulseFit (Heka Elektronic), MiniAnalysis (Synaptosoft, Georgia, USA), and Origin (Origin Laboratories, Northampton, MA, USA) software. MiniAnalysis was used to detect spontaneous synaptic events and generated most of the parameters that were used in the analyses. To quantify IPSCs, we integrated the area of individual IPSCs within specified bins to determine the total synaptic charge (Q; pA ms). This measure captures changes in both the frequency and the amplitude of synaptic events. For voltage clamp recordings, DSI was analysed by comparing the Q of all events in a 10 s bin before depolarization with the Q during a 10 s bin after depolarization. The first 2 s following the voltage step were disregarded to allow maximal DSI to develop. The percentage charge suppression (i.e. DSI) was calculated as: $DSI = [1 - (Q_{post}/Q_{pre})] \times 100$. Therefore, a value of 78 indicates a 78% decrease in Q following the depolarizing voltage step. For current clamp recordings, baseline sIPSP activity was calculated by averaging the total area in a 10 s bin prior to delivery of the action potential train. Each 5 s bin immediately following the train was then compared to baseline using the above equation (substituting area for charge). Amplitude distributions for sIPSCs were tested for significance using Kolmogorov-Smirnov statistics (K-S). All other data were compared using repeated measures ANOVAs or Student's paired t tests and presented as mean ± S.E.M.

Results

Somatic, whole-cell voltage clamp recordings were obtained from a total of 123 PNs located in layer 2/3 of mouse auditory and visual cortices. In a subset of cells tested with both the $GABA_A$ antagonist bicuculline methiodide (BIC; 30 μM) and TTX, the baseline sIPSC frequency in the absence of drug was 3.3 ± 0.5 Hz (n = 6). These events were completely abolished by BIC and partially suppressed by TTX (1 μM; 37.4% of baseline), indicating that the sIPSCs are $GABA_A$-mediated synaptic currents comprising both action potential-dependent and -independent events.

Recently we have shown that DSI of evoked IPSCs in the neocortex is mediated by activation of presynaptic CB1Rs on GABAergic interneurones (Trettel & Levine, 2003), similar to the hippocampus and the cerebellum (Kreitzer & Regehr, 2001; Wilson & Nicoll, 2001; Diana *et al.* 2002; Yoshida *et al.* 2002). Moreover, CB1R mRNA expression in the neocortex is mostly restricted to a specific class of interneurones that synthesize CCK (Marsicano & Lutz, 1999). Because muscarinic receptor activation has been shown to directly depolarize CCK-expressing interneurones in the neocortex (Kawaguchi, 1997), we used the cholinergic agonist carbamylcholine chloride (CCh) to elevate the spontaneous activity of these cells. As shown in the example in Fig. 1*A*, bath application of CCh (5 μM) produced a 4-fold increase in sIPSC charge (Fig. 1*B*; $P < 0.05$; $n = 6$). The effect of CCh was blocked by atropine (2 μM; data not shown), indicating that muscarinic receptor activation was responsible. To verify that CCh increased the activity of CB1R-containing cells, we bath-applied an exogenous cannabinoid during CCh exposure. In the presence of WIN55,212-2 (5 μM), sIPSC charge dropped to 43 ± 5.5% of the CCh baseline (Fig. 1*A* and *B*; $P < 0.05$; $n = 6$), which was not significantly different from the mean charge prior to the addition of CCh. These data indicate that a majority of CCh-sensitive interneurones express CB1R.

The increase in sIPSCs in response to cholinergic stimulation is most likely due to increased action potential

(AP) activity in a subset of interneurones (Martin & Alger, 1999; Kondo & Kawaguchi, 2001). To determine whether CCh had direct synaptic effects that could also contribute to the increase in sIPSC charge, we recorded AP-independent IPSCs (miniature IPSCs, or mIPSCs). Exposure to TTX (1 μM) caused a significant decrease in charge, due to a decrease in sIPSC frequency, and subsequent exposure to CCh had no effect on the mIPSCs (Fig. 1*C* and *D*; $n = 6$). These data indicate that the IPSCs induced by CCh were action potential-dependent events, and also suggest that CCh does not have any direct presynaptic effects on transmitter release under our experimental conditions.

Depolarization-induced suppression of sIPSCs

In the presence of CCh, PN depolarization (–70 to 0 mV; 1 s) caused a dramatic and transient suppression of sIPSCs (i.e. DSI; Fig. 2*A* and *D*). The distribution of sIPSC amplitudes in the presence of CCh revealed the presence of a newly recruited population of inputs that had large amplitudes and were selectively eliminated after the post-synaptic voltage step (Fig. 2*B*, compare baseline and post DSI distributions). In a group of eight cells, the mean value of DSI was 71.6 ± 3.4% (Fig. 2*E*, $P < 0.05$). We next examined whether endocannabinoids mediated the suppression of CCh-stimulated sIPSCs. The effect of the PN voltage step on synaptic currents was blocked when the CB1R antagonist AM251 (5 μM) was present (Fig. 2*C*, *D* and *E*; $n = 5$). As illustrated in Fig. 2*D*, no significant change in sIPSC charge occurred following the voltage step in the presence of AM251, whereas significant suppression in control cells lasted for ~18 s. AM251 alone had no effect on sIPSC charge (data not shown). Similarly, if the suppression of sIPSCs required CB1R signalling then activation of CB1R with an exogenous agonist should occlude the effects of depolarization. As shown in Fig. 2*E*, preincubation of the brain slices in ACSF containing the cannabinoid receptor agonist WIN55,212-2 (5 μM) blocked DSI ($n = 9$).

One possibility is that DSI requires cholinergic stimulation, because application of CCh in the hippocampus has been shown to directly enhance endocannabinoid synthesis by PNs (Kim *et al.* 2002). Therefore, we wanted to determine whether DSI occurred in the absence of CCh. In fact, significant DSI could still be obtained (10.9 ± 6%; $P < 0.05$; $n = 11$), although the magnitude of DSI was greatly reduced compared to that seen in the presence of CCh. This modest level of DSI in control conditions could be attributed to the low basal rate of interneurone discharge *in vitro*, i.e. a paucity of sIPSCs. To further explore the specificity of CCh in activating DSI-sensitive interneurones, we also used the group I/II metabotropic glutamate receptor (mGluR) agonist (1*S*,3*R*)-ACPD (75 μM) to preferentially excite somatostatin-expressing, low threshold spiking interneurones (Beierlein *et al.* 2000). ACPD caused a 10-fold increase in sIPSC frequency. However, despite this dramatic increase in activity, the magnitude of DSI was not different from control conditions (8.3 ± 1.1%; $n = 5$),

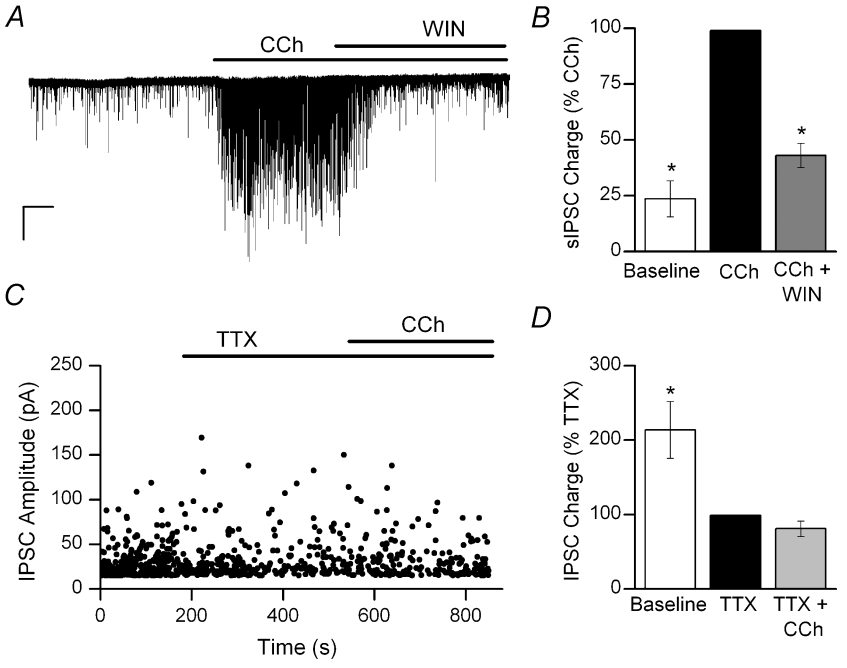

Figure 1. Spontaneous inhibitory inputs recruited by carbachol (CCh) application are sensitive to exogenous cannabinoids
A, representative current trace showing the effect of CCh (5 μM) and subsequent CB1R activation by the aminoalkylindole WIN55,212-2 (WIN; 5 μM) on sIPSCs. Scale bars: 200 pA, 45 s. *B*, group data illustrating the changes in sIPSC charge during CCh and CCh + WIN conditions ($n = 6$). Data are normalized to the CCh baseline. *C*, addition of CCh does not alter the frequency or amplitude of miniature IPSCs recorded in the presence of tetrodotoxin (TTX; 1 μM). *D*, group data for the effect of CCh on miniature IPSC charge ($n = 6$). The data are normalized to the TTX condition. *$P < 0.05$.

suggesting that interneurones activated by ACPD were not DSI sensitive.

Because other metabotropic signalling systems have also been implicated in DSI, we explored the involvement of mGluR and $GABA_B$ receptor activation in the endocannabinoid-mediated suppression of sIPSCs. Blocking group I and II mGluRs with a cocktail of the group II antagonist LY341495 (75 μM) and the mixed group I/II antagonist MCPG (1 mM) resulted in DSI that was not significantly different from DSI in the presence of CCh (Fig. 2*E* and 60.2 ± 4.8%; $n = 7$). Similarly, blocking $GABA_B$ receptors with the high affinity antagonist CGP35348 (65 μM) also did not change the magnitude of DSI compared to CCh alone (Fig. 2*E* and 65.3 ± 7%, $n = 5$). These data confirm that CB1R activation is required for sIPSC suppression and neither mGluR nor $GABA_B$ receptor activation contribute to the induction or expression of endocannabinoid-mediated DSI in the neocortex under these conditions.

Induction of DSI by action potentials

We next asked whether a train of APs, rather than sustained membrane depolarization, could lead to a suppression of inhibition. For these experiments, APs were evoked at 20 Hz, a frequency that is similar to the PN firing rates observed *in vivo* (Steriade, 2000). Under current clamp conditions, adding CCh to the bath sharply increased the frequency of $GABA_A$-mediated spontaneous inhibitory postsynaptic potentials (sIPSPs) from 1.77 ± 0.3 to 4.85 ± 0.5 Hz (data not shown; $P < 0.05$; $n = 7$). Following a

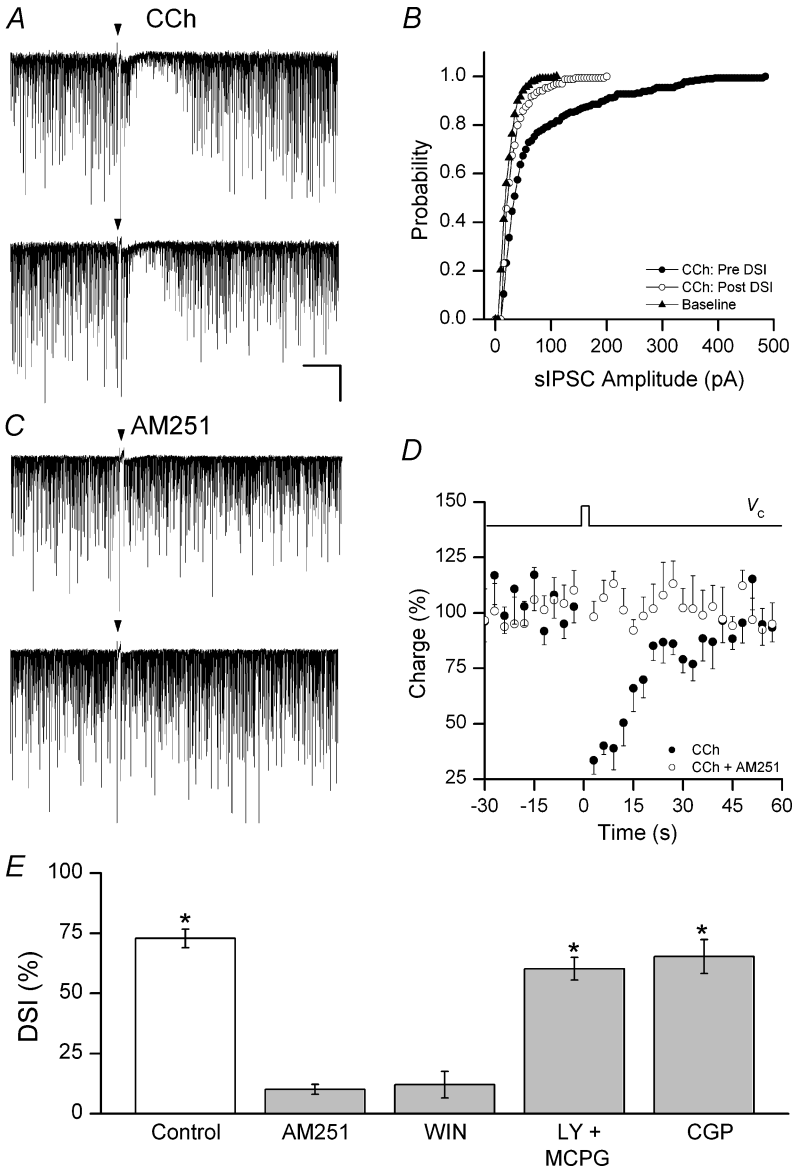

Figure 2. Depolarization-induced suppression of sIPSCs is mediated by endocannabinoid signalling
A, representative traces of DSI in the presence of carbachol (CCh; 5 μM). Spontaneous synaptic currents were recorded from layer 2/3 PNs and DSI was induced by a 1 s depolarization step to 0 mV (arrowheads). Scale bars for *A* and *C*: 250 pA, 7 s. *B*, cumulative probability plot for a single neurone illustrating the effects of the voltage step on sIPSC amplitudes. For comparison, the baseline data represent the sIPSCs recorded prior to the addition of CCh to the bath ACSF. Bin width = 10 s. *C*, representative traces showing the lack of DSI in the presence of the selective CB1R antagonist AM251 (5 μM). *D*, group time course plotting sIPSC charge for the CCh and CCh + AM251 conditions. The command voltage (V_c) is represented at the top of the graph. *E*, group data for DSI in the presence of CCh (5 μM). Data are shown for control ($n = 8$), and during treatment with the CB1R antagonist AM251 (5 μM; $n = 5$), the cannabinoid agonist WIN55,212 2 (WIN; 5 μM; $n = 9$), the metabotropic glutamate receptor antagonists LY341495 (LY; 65 μM) plus MCPG (1 mM; $n = 7$), and the $GABA_B$ receptor antagonist CGP55845 (CGP; 75 μM; $n = 5$). *$P < 0.05$.

single 20 Hz AP train (train duration = 1 s), sIPSP area was suppressed by 89 ± 2.3% during the 5 s period following the AP train and returned to baseline levels within 15–20 s (Fig. 3*A* and *D*; $P < 0.05$; $n = 6$). Similar to the results obtained in voltage clamp, the AP train induced a marked suppression of large amplitude sIPSPs (Fig. 3*C*). To determine if the suppression of sIPSPs was mediated by the release of endocannabinoids, we bath-applied a CB1R antagonist. In the presence of AM251 (5 μM), the AP train failed to induce significant sIPSP suppression (Fig. 3*B* and *D* and 8.0 ± 9.8%; $n = 6$).

Spatial distribution of suppressed sIPSCs

The spatial location of an inhibitory synapse on a target neurone will partly determine the roles that that synapse, and hence that presynaptic neurone, will play in influencing the activity and synaptic integration properties of the postsynaptic cell. In order to resolve the approximate location of DSI-susceptible synapses, we used focal application of the $GABA_A$ antagonist BIC to isolate distinct domains of the PN membrane. Neurones used for these experiments were located deep in layer 3 and had clearly visible apical dendrites extending into layer 1. To validate this experimental approach, GABA was iontophoretically applied at the perisomatic and distal apical dendritic regions, while BIC was applied close to the soma (Fig. 4*A*). Consistent with electrotonic decay, the slope and amplitude of the GABA current (I_{GABA}) progressively decreased as the iontophoretic electrode was moved from the soma towards the distal apical dendrite (see example in Fig. 4*B*). However, the contribution of site-dependent heterogeneity in $GABA_A$ receptor subunit expression to the difference in slope and amplitude of I_{GABA} cannot be ruled out. On average, the amplitude of the somatic I_{GABA} was 2.63 ± 1.11 nA ($n = 4$) compared to 0.45 ± 0.17 nA ($n = 4$) for the dendritic I_{GABA} elicited >80 μm distal from the soma. After obtaining stable I_{GABA} at both locations, BIC was ejected onto the soma. As shown in Fig. 4*C*, BIC application abolished the perisomatic I_{GABA} (4.2 ± 2.1% of baseline; $n = 4$) but had no effect on dendritic I_{GABA} (96.2 ± 3% of baseline; $n = 4$). These results demonstrate that $GABA_A$ receptors and presumably GABAergic inputs on the apical dendrite can be isolated

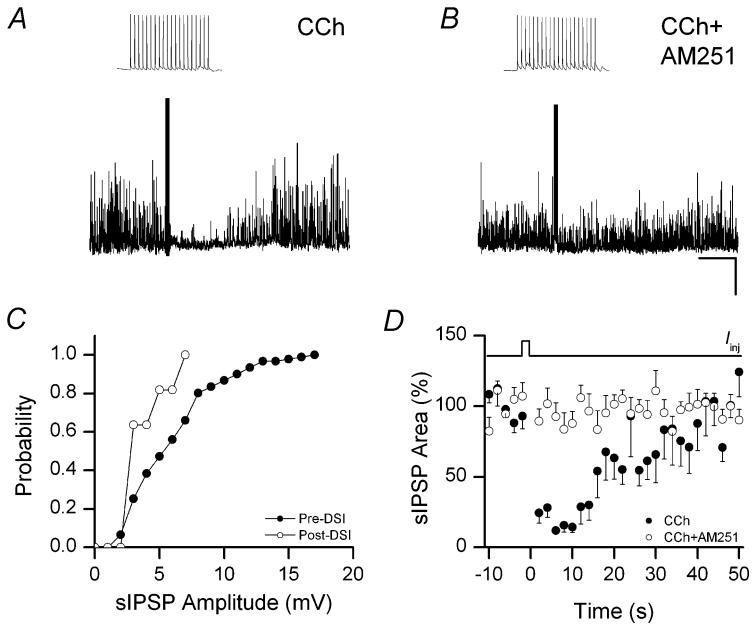

Figure 3. Suppression of sIPSP activity following a brief train of action potentials (APs) is mediated by the release of endocannabinoids

A, whole-cell current clamp recording from a layer 2/3 PN demonstrating AP-induced DSI in the presence of CCh (5 μM). The AP train was delivered at 20 Hz for 1 s. *B*, the AP-induced suppression is blocked by bath application of the CB1R antagonist AM251 (5 μM). Action potential amplitudes in both *A* and *B* are truncated for clarity and the AP train is shown above each trace on an expanded time scale. Traces shown in *A* and *B* were recorded from the same cell. Scale bars for *A* and *B*: 5 mV, 10 s (inset: 60 mV, 500 ms). *C*, cumulative amplitude histogram characterizing sIPSPs in 20 s bins prior to and following delivery of the AP train. *D*, group data ($n = 6$) illustrating the time course of AP-induced DSI in the presence and absence of AM251. The current injection (I_{inj}) used to induce APs is represented at the top of the graph.

from those on and near the soma by focally applying BIC.

To analyse the spatial distribution of the synapses suppressed by PN depolarization, we applied BIC to either the perisomatic or apical dendritic areas in the presence of CCh. We assessed changes in sIPSC frequency rather than charge because it provided a more sensitive measure of the effects of dendritic BIC application. As shown in Fig. 4*D* and *E*, somatic application of BIC appeared to mimic the effects of DSI, significantly reducing sIPSC frequency. Dendritic application of BIC was also effective in blocking a subset of spontaneous inhibitory inputs, as it produced a significant decrease in sIPSC frequency (Fig. 4*E*). Because dendritic BIC blocked smaller amplitude sIPSCs, the effect is not readily seen in the compressed time scale of Fig. 4*A* (but see Fig. 5*C*).

A typical distribution of baseline sIPSC amplitudes is shown in the top panel of Fig. 5*A*. Depolarization produced a significant decrease in the frequency of sIPSCs and a shift in the amplitude distribution (Fig. 5*A*, middle and bottom panels). Examining the amplitude histograms from individual experiments revealed a selective loss of large amplitude sIPSCs, resulting in a shift towards smaller amplitude events ($P < 0.05$, 8/8 cells; K-S test). Because GABAergic inputs to the soma of PNs produce larger somatic currents than do dendritic inputs (Miles *et al.* 1996), the loss of large sIPSCs is consistent with a perisomatic localization for the DSI-susceptible inputs. Focally applying BIC to the PN soma produced results that were virtually identical to the results obtained during DSI (Fig. 5*A versus B*). Somatic BIC significantly reduced sIPSC frequency (Fig. 4*E*) and shifted the amplitude distribution towards smaller events (Fig. 5*B*), an effect that was consistently seen in all cells tested ($P < 0.05$, 8/8 cells; K-S test). Application of BIC in the apical dendritic region also produced a significant decrease in sIPSC frequency (Figs 4*E* and 5*C*). However, in contrast to both DSI and somatic BIC, apical BIC shifted the amplitude distribution

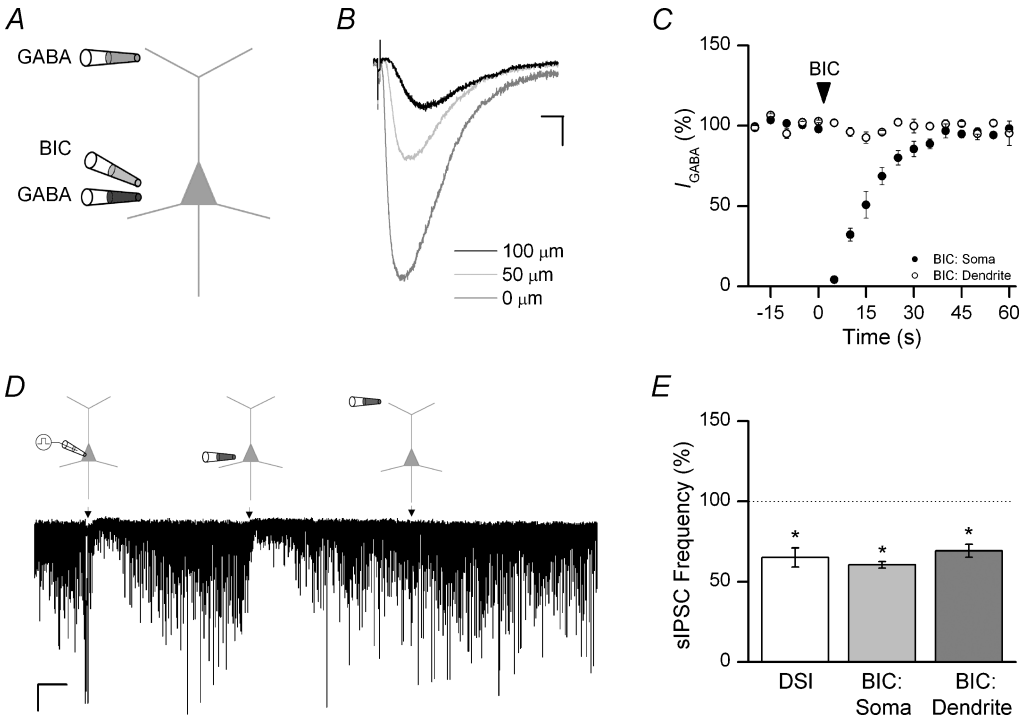

Figure 4. The effects of DSI and focal bicuculline application on sIPSCs

A, experimental setup for isolating $GABA_A$ receptors on the apical dendritic and perisomatic membrane. The illustration shows micropipette placement used to eject bicuculline (BIC, 150 μM) and GABA (100 μM) onto a layer 3 PN. *B*, GABA currents (I_{GABA}) elicited by iontophoretic ejection of GABA onto PNs at variable distances along the apical dendrite. The distance *x* indicated in the figure represents the distance from the centre of the soma to the site of drug ejection. Scale bars: 150 pA, 25 ms. *C*, pressure ejection of BIC onto the soma transiently abolished the somatic I_{GABA} but did not affect the amplitude of dendritic I_{GABA} ($x = 75$ μm). GABA currents were elicited at 0.2 Hz. *D*, example time course of sIPSCs recorded from a single PN during DSI (left arrowhead; 0 mV for 1 s), somatic BIC application (middle arrowhead), and dendritic BIC application (right arrowhead). Scale bars: 75 pA, 10 s. *E*, mean sIPSC frequency for each of the aforementioned conditions ($n = 6$ cells for each condition). $^*P < 0.05$.

in the opposite direction by selectively depressing small amplitude sIPSCs (Fig. 5*C*; $P < 0.05$, 5/8 cells; K-S test).

The kinetics of sIPSCs will change systematically as a function of distance from the recording pipette due to the electronic properties of the neural membrane (Segev & London, 1999). Therefore, we also analysed sIPSC rise times (10–90%) in the same set of cells presented in Fig. 5. The somatic voltage step (DSI) shifted the rise time distribution towards slower sIPSCs (Fig. 6*A*), producing a significant increase in the mean rise time (Fig. 6*D* and 119.4 ± 6.6% of baseline; $P < 0.05$, $n = 8$). Somatic BIC produced a similar change in sIPSC rise times, increasing the mean value to 136.4 ± 7.4% of baseline (Fig. 6*B* and *D*; $P < 0.05$, $n = 8$). In contrast, apical BIC selectively blocked sIPSCs with slow rise times, significantly reducing the mean to 88.4 ± 3.2% of baseline (Fig. 6*C* and *D*; $P < 0.05$; $n = 8$). The preservation of sIPSCs with fast rise times (typically less than 2 ms) indicates that dendritic BIC selectively blocked inputs to the apical dendrites.

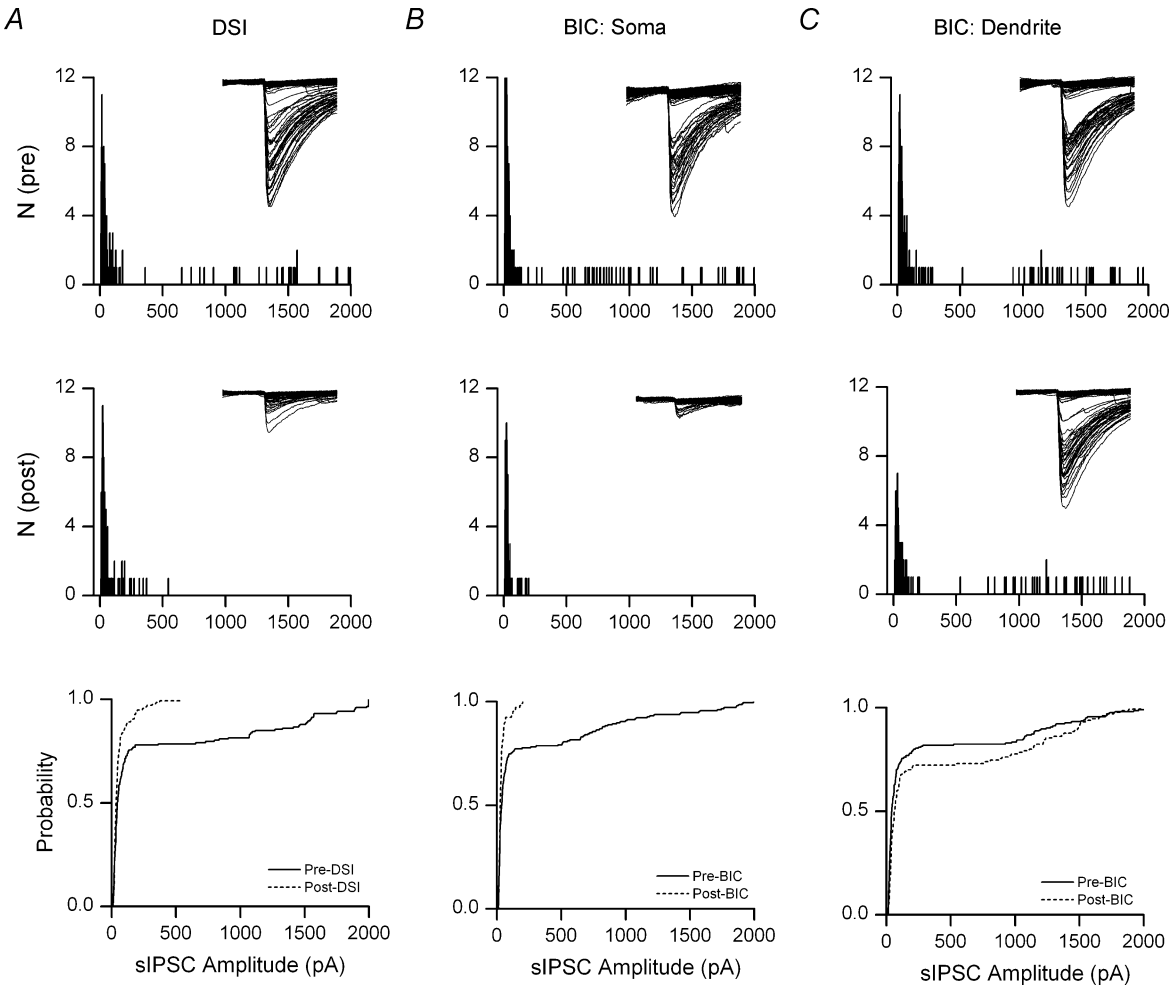

Figure 5. Somatic, but not dendritic, bicuculline (BIC) mimics the effect of DSI on sIPSC amplitude distributions

A, amplitude histograms of sIPSCs before (top panel) and after (middle panel) a 1 s depolarizing voltage step (DSI). The insets in each distribution are the individual sweeps that were used to construct the distributions. The bottom panel shows the cumulative probability plot of the sIPSCs before and after somatic depolarization. *B*, amplitude histograms before (top) and after (middle) BIC was focally applied to the somatic membrane. The cumulative probability plot for the cell is shown in the bottom panel. *C*, Amplitude histograms before (top) and after (middle) BIC was focally applied to the distal dendritic membrane. The cumulative probability plot for dendritic BIC application is shown in the bottom panel. Note the selective loss of large amplitude events in *A* and *B*, and the loss of only small amplitude events in *C*. Histogram bin width = 5 pA. All data are from the same neurone and the analysis windows for each condition were 10 s pre- and post-treatment; carbachol (5 μM) was present throughout. Group data and statistical comparisons are reported in Results.

Taken together, these data suggest that DSI preferentially suppressed synapses that target the perisomatic membrane of PNs.

The above results suggest that apical GABAergic inputs are not sensitive to endocannabinoid-mediated DSI. However, there may be a population of CB1R-expressing afferents that target apical dendrites but are not activated by CCh. This could explain the lack of effect of DSI on apical inputs. In a separate set of experiments we elevated extracellular K^+ to 12 mM to increase sIPSC activity without preference for a specific class of interneurones. Under these conditions, DSI still resulted in a significant suppression of large amplitude events (not shown) and an increase in mean rise time (Fig. 6*D*), suggesting preferential suppression of somatic inputs. Another possibility is that at least some active apical inputs express CB1R but the depolarization step used does not result in endocannabinoid release from apical dendrites. However, bath application of the cannabinoid agonist WIN55,212-2 (5 μM) significantly increased mean rise time in the presence or absence of carbachol (data not shown), suggesting that apical inputs were not affected by CB1R activation.

Discussion

Several recent studies have demonstrated that DSI in the hippocampus and cerebellum is mediated by the release of endocannabinoids (Kreitzer & Regehr, 2001; Ohno-Shosaku *et al.* 2001; Wilson & Nicoll, 2001). These lipid-derived messengers are released from postsynaptic cells and act retrogradely to inhibit GABA release from presynaptic terminals. We have recently demonstrated a similar phenomenon for interneurone to pyramidal neurone synapses of the neocortex using evoked inhibitory synaptic currents (Trettel & Levine, 2003). In the present study, we examined DSI of spontaneous rather than evoked inhibitory inputs to PNs in order to determine the cellular specificity of neocortical endocannabinoid signalling as well as the location of cannabinoid-sensitive synaptic inputs.

Our first goal was to establish whether a specific subclass of inhibitory afferents to layer 2/3 PNs are susceptible to DSI. Pyramidal neurones are innervated by several distinct types of interneurones that form synapses on segregated domains of the target PN. Under baseline conditions, significant suppression of inhibition was observed, but only a fraction of the spontaneous synaptic currents appeared to be affected. Since muscarinic receptor activation has been shown to selectively depolarize CCK-expressing (and presumably CB1R-expressing) interneurones (Kawaguchi, 1997), we bath-applied CCh in order to increase the firing rate of these interneurones. Similar to results obtained in the hippocampus (e.g. Martin *et al.* 2001) and frontal cortex (Kondo & Kawaguchi, 2001), carbachol greatly increased sIPSC activity in sensory neocortex. In particular, CCh increased AP-dependent activity in a subpopulation of afferents that generated large amplitude synaptic currents with rapid rise times. Furthermore, the inputs

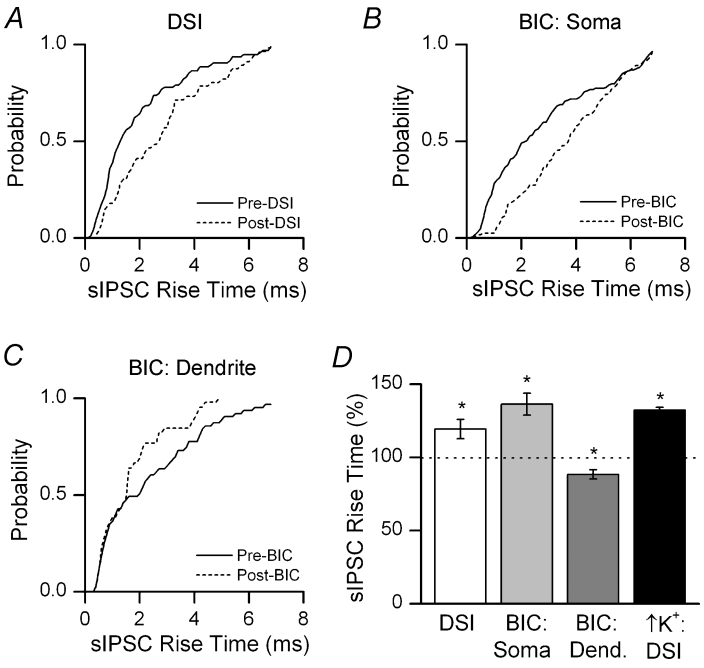

Figure 6. Analysis of sIPSC rise times reveals a loss of somatic currents during DSI

A-C, cumulative probability plots of sIPSC rise times (10–90%) during the 10 s windows before and after membrane depolarization (*A*), somatic BIC (*B*), and dendritic BIC (*C*). *D*, mean sIPSC rise times for DSI ($n = 6$), somatic BIC ($n = 6$), dendritic BIC ($n = 6$) and DSI in the presence of 12 mM $[K^+]_o$ ($n = 3$). Carbachol (5 μM) was present throughout with the exception of the elevated K^+ condition. $^*P < 0.05$.

recruited by CCh were particularly susceptible to DSI – these currents were almost completely inhibited in response to postsynaptic depolarization. This effect was mediated by release of an endocannabinoid because it was blocked by a CB1R antagonist and occluded by a CB1R agonist. Moreover, DSI was unaffected by antagonists to metabotropic glutamate and GABA receptors. It is also important to note that muscarinic receptor activation, besides increasing interneurone firing, may enhance endocannabinoid production (Kim *et al.* 2002), and this may play a role in the enhanced DSI seen in the presence of CCh.

As most studies of DSI have used prolonged depolarization to induce suppression, the physiological relevance of this phenomenon is unclear. In the hippocampus, there have been conflicting reports regarding the ability of AP trains to induce DSI (Pitler & Alger, 1992; Ohno-Shosaku *et al.* 2001; Hampson *et al.* 2003). We therefore asked whether APs were sufficient to elicit DSI in the neocortex. We found that cortical DSI was reliably induced with a 20 Hz train of action potentials. This AP-triggered DSI was blocked by a CB1R antagonist, indicating that it was mediated by the release of an endocannabinoid. These results suggest that physiologically relevant levels of action potential firing alone are capable of inducing endocannabinoid-mediated DSI in the neocortex. The magnitude and duration of DSI caused by a 1 s train of APs at 20 Hz was similar to that seen using a 1 s depolarization to 0 mV. Thus, it may be possible to use more physiological induction parameters to address questions about the functional role of DSI in synaptic transmission. Further studies are needed to determine the minimal, or threshold level of activity required to induce endocannabinoid release in the cortex, as well as to address potential differences between cortical and hippocampal DSI with regard to AP induction.

We next investigated the spatial distribution of DSI-susceptible synaptic inputs to layer 2/3 PNs. Anatomical studies have shown that expression of CB1R in the neocortex, as well as in the hippocampus, is mostly limited to GABAergic interneurones that express CCK (Marsicano & Lutz, 1999; Egertova & Elphick, 2000). CCK-positive GABAergic interneurones are basket cells, typically forming synapses on the soma and proximal dendrites of PN targets. In the present studies, we found that the synaptic currents suppressed by depolarization had faster rise times and larger amplitudes than the currents that were not suppressed, suggesting a perisomatic localization. These results are similar to those obtained in the hippocampus (Martin *et al.* 2001; Wilson *et al.* 2001).

We also directly examined the spatial distribution of these afferents using local application of the $GABA_A$ antagonist BIC. By applying BIC focally at either the soma or apical dendrites, we were able to clearly separate inhibitory somatic events from inhibitory dendritic events. When applied at the pyramidal cell soma, BIC preferentially suppressed large, fast IPSCs, similar to the effects of depolarization. Conversely, application of the antagonist in the apical dendrites of PNs suppressed small, slow currents, similar to the sIPSCs that were generally unaffected during DSI. Thus, both somatic and dendritic BIC were effective in blocking distinct populations of inhibitory inputs, but only somatic BIC mimicked the effects of DSI. Taken together, these studies provide evidence that depolarization-induced cannabinoid release selectively suppresses GABA release from perisomatic inhibitory afferents. These cells most likely constitute a class of CCK/CB1R-expressing basket cells.

What are the functional implications of selectively suppressing perisomatic inhibition? Inhibitory synapses on different domains of PNs in both cortex and hippocampus modulate distinct aspects of activity (Soltesz *et al.* 1995; Miles *et al.* 1996; Somogyi *et al.* 1998; Larkum *et al.* 1999; Williams & Stuart, 2003). Synapses on or near the axon hillock can directly modulate action potential generation by providing a high conductance current shunt near the site of summation. Other inhibitory inputs that target distal dendrites can influence neuronal responsiveness to excitatory inputs by modulating the local membrane potential and altering the passive membrane properties by dynamically changing the local membrane conductance. Inhibitory somatic inputs, on the other hand, provide potent and tonic inhibition that can regulate action potential timing by effectively blocking the spread of depolarization towards the hillock. Somatic inhibition could also regulate the back-propagation of action potentials into the dendritic arbor; back-propagation in PNs is critical for synaptic integration and plasticity as well as burst mode firing (Larkum *et al.* 1999). Therefore, a function of endocannabinoid-mediated DSI in the neocortex may be to alter the integrative properties of PNs by selectively and potently removing one form of somatic inhibition.

Modulation of CCK release may also mediate some of the physiological effects of cannabinoids. The CB1R-expressing interneurones presumably use CCK as a cotransmitter, and potassium-evoked CCK release in the hippocampus is inhibited by CB1R activation (Beinfeld & Connolly, 2001). There is also evidence that the release of CCK and GABA can be differentially regulated in presynaptic terminals (reviewed in Ghijsen *et al.* 2001),

thus it could be important to compare the effects of CB1R activation on the release of each transmitter under various physiological conditions. Little is known about the cellular effects of activating the CCK-B receptor in neurones, but CCK may decrease postsynaptic firing by stimulating A-type potassium channels (Burdakov & Ashcroft, 2002). CCK and cannabinoids appear to have contrasting roles in several brain functions, including spatial memory (Jentsch *et al.* 1997; Sebret *et al.* 1999; Beinfeld & Connolly, 2001), supporting the idea that some of the effects of cannabinoids may result from decreased CCK release.

Because retrograde endocannabinoid signalling appears to regulate a specific class of inhibitory inputs, it may be interesting to examine whether other classes of inputs to pyramidal cells can also be modulated by retrograde signalling. It has been shown, for example, that dendritic glutamate release suppresses the activity of fast spiking interneurones in the neocortex (Zilberter, 2000). These fast spiking cells preferentially target the dendritic membrane of PNs (Kawaguchi & Kubota, 1996) and are thought to play a role in synaptic integration (Somogyi *et al.* 1998). Thus, different patterns of PN firing may release retrograde signals from either the soma or dendrites, thereby shifting the focus of inhibition from one cellular compartment to another.

Overall, the present results indicate that cortical PNs release endocannabinoids in response to depolarizing stimuli, including short trains of action potentials. Endocannabinoids act in a retrograde manner to suppress GABA release from presynaptic terminals, specifically targeting perisomatic afferents that presumably arise from CCK-expressing interneurones. The selective suppression of these inputs by endocannabinoids would likely have important functional consequences for PN processing and therefore, the output of the neocortex.

References

Beierlein M, Gibson JR & Connors BW (2000). A network of electrically coupled interneurons drives synchronized inhibition in neocortex. *Nat Neurosci* **3**, 904–910.

Beinfeld MC & Connolly K (2001). Activation of CB1 cannabinoid receptors in rat hippocampal slices inhibits potassium-evoked cholecystokinin release, a possible mechanism contributing to the spatial memory defects produced by cannabinoids. *Neurosci Lett* **301**, 69–71.

Burdakov D & Ashcroft FM (2002). Cholecystokinin tunes firing of an electrically distinct subset of arcuate nucleus neurons by activating A-type potassium channels. *J Neurosci* **22**, 6380–6387.

Chevaleyre V & Castillo PE (2003). Heterosynaptic LTD of hippocampal GABAergic synapses: a novel role of endocannabinoids in regulating excitability. *Neuron* **38**, 461–472.

Connors BW & Gutnick MJ (1990). Intrinsic firing patterns of diverse neocortical neurons. *Trends Neurosci* **13**, 99–104.

Diana MA, Levenes C, Mackie K & Marty A (2002). Short-term retrograde inhibition of GABAergic synaptic currents in rat Purkinje cells is mediated by endogenous cannabinoids. *J Neurosci* **22**, 200–208.

Di Marzo V, Melck D, Bisogno T & De Petrocellis L (1998). Endocannabinoids: endogenous cannabinoid receptor ligands with neuromodulatory action. *Trends Neurosci* **21**, 521–528.

Egertova M & Elphick MR (2000). Localisation of cannabinoid receptors in the rat brain using antibodies to the intracellular C-terminal tail of CB. *J Comp Neurol* **422**, 159–171.

Ferraro L, Tomasini MC, Cassano T, Bebe BW, Siniscalchi A, O'Connor WT, Magee P, Tanganelli S, Cuomo V & Antonelli T (2001). Cannabinoid receptor agonist WIN 55,212-2 inhibits rat cortical dialysate gamma-aminobutyric acid levels. *J Neurosci Res* **66**, 298–302.

Freund TF, Katona I & Piomelli D (2003). Role of endogenous cannabinoids in synaptic signaling. *Physiol Rev* **83**, 1017–1066.

Frisina R & Walton J (2001). Neuroanatomy of the central auditory system. In *Handbook of Mouse Auditory Research: from Behavior to Molecular Biology*, ed. Willott, J., pp. 243–277. CRC Press, Boca Raton.

Gerdeman GL, Ronesi J & Lovinger DM (2002). Postsynaptic endocannabinoid release is critical to long-term depression in the striatum. *Nat Neurosci* **5**, 446–451.

Ghijsen WE, Leenders AG & Wiegant VM (2001). Regulation of cholecystokinin release from central nerve terminals. *Peptides* **22**, 1213–1221.

Gupta A, Wang Y & Markram H (2000). Organizing principles for a diversity of GABAergic interneurons and synapses in the neocortex. *Science* **287**, 273–278.

Hampson RE, Zhuang SY, Weiner JL & Deadwyler SA (2003). Functional significance of cannabinoid-mediated, depolarization-induced suppression of inhibition (DSI) in the hippocampus. *J Neurophysiol* **90**, 55–64.

Jentsch JD, Andrusiak E, Tran A, Bowers MB Jr & Roth RH (1997). Delta 9-tetrahydrocannabinol increases prefrontal cortical catecholaminergic utilization and impairs spatial working memory in the rat: blockade of dopaminergic effects with HA966. *Neuropsychopharmacology* **16**, 426–432.

Katona I, Sperlagh B, Sik A, Kafalvi A, Vizi ES, Mackie K & Freund TF (1999). Presynaptically located CB1 cannabinoid receptors regulate GABA release from axon terminals of specific hippocampal interneurons. *J Neurosci* **19**, 4544–4558.

Kawaguchi Y (1997). Selective cholinergic modulation of cortical GABAergic cell subtypes. *J Neurophysiol* **78**, 1743–1747.

Kawaguchi Y & Kubota Y (1996). Physiological and morphological identification of somatostatin- or vasoactive intestinal polypeptide-containing cells among GABAergic cell subtypes in rat frontal cortex. *J Neurosci* **16**, 2701–2715.

Kawaguchi Y & Kubota Y (1997). GABAergic cell subtypes and their synaptic connections in rat frontal cortex. *Cereb Cortex* **7**, 476–486.

Kawaguchi Y & Kubota Y (1998). Neurochemical features and synaptic connections of large physiologically-identified GABAergic cells in the rat frontal cortex. *Neuroscience* **85**, 677–701.

Kim J, Isokawa M, Ledent C & Alger BE (2002). Activation of muscarinic acetylcholine receptors enhances the release of endogenous cannabinoids in the hippocampus. *J Neurosci* **22**, 10182–10191.

Kondo S & Kawaguchi Y (2001). Slow synchronized bursts of inhibitory postsynaptic currents (0.1–0.3 Hz) by cholinergic stimulation in the rat frontal cortex in vitro. *Neuroscience* **107**, 551–560.

Kreitzer AC & Regehr WG (2001). Cerebellar depolarization-induced suppression of inhibition is mediated by endogenous cannabinoids. *J Neurosci* **21**, RC174.

Kubota Y & Kawaguchi Y (1997). Two distinct subgroups of cholecystokinin-immunoreactive cortical interneurons. *Brain Res* **752**, 175–183.

Larkum ME, Zhu JJ & Sakmann B (1999). A new cellular mechanism for coupling inputs arriving at different cortical layers. *Nature* **398**, 338–341.

Llano I, Leresche N & Marty A (1991). Calcium entry increases the sensitivity of cerebellar Purkinje cells to applied GABA and decreases inhibitory synaptic currents. *Neuron* **6**, 565–574.

Marsicano G & Lutz B (1999). Expression of the cannabinoid receptor CB1 in distinct neuronal subpopulations in the adult mouse forebrain. *Eur J Neurosci* **11**, 4213–4225.

Marsicano G, Wotjak CT, Azad SC, Bisogno T, Rammes G, Cascio MG, Hermann H, Tang J, Hofmann C, Zieglgansberger W, Di Marzo V & Lutz B (2002). The endogenous cannabinoid system controls extinction of aversive memories. *Nature* **418**, 530–534.

Martin LA & Alger BE (1999). Muscarinic facilitation of the occurrence of depolarization-induced suppression of inhibition in rat hippocampus. *Neuroscience* **92**, 61–71.

Martin LA, Wei DS & Alger BE (2001). Heterogeneous susceptibility of $GABA_A$ receptor-mediated IPSCs to depolarization-induced suppression of inhibition in rat hippocampus. *J Physiol* **532**, 685–700.

McCormick DA, Connors BW, Lighthall JW & Prince DA (1985). Comparative electrophysiology of pyramidal and sparsely spiny stellate neurons of the neocortex. *J Neurophysiol* **54**, 782–806.

Miles R, Toth K, Gulyas AI, Hajos N & Freund TF (1996). Differences between somatic and dendritic inhibition in the hippocampus. *Neuron* **16**, 815–823.

Ohno-Shosaku T, Maejima T & Kano M (2001). Endogenous cannabinoids mediate retrograde signals from depolarized postsynaptic neurons to presynaptic terminals. *Neuron* **29**, 729–738.

Paxinos G & Franklin KBJ (2001). *The Mouse Brain in Stereotaxic Coordinates*. Academic Press, San Diego.

Pitler TA & Alger BE (1992). Postsynaptic spike firing reduces synaptic $GABA_A$ responses in hippocampal pyramidal cells. *J Neurosci* **12**, 4122–4132.

Pitler TA & Alger BE (1994). Depolarization-induced suppression of GABAergic inhibition in rat hippocampal pyramidal cells: G protein involvement in a presynaptic mechanism. *Neuron* **13**, 1447–1455.

Robbe D, Kopf M, Remaury A, Bockaert J & Manzoni OJ (2002). Endogenous cannabinoids mediate long-term synaptic depression in the nucleus accumbens. *Proc Natl Acad Sci U S A* **99**, 8384–8388.

Sebret A, Lena I, Crete D, Matsui T, Roques BP & Dauge V (1999). Rat hippocampal neurons are critically involved in physiological improvement of memory processes induced by cholecystokinin-B receptor stimulation. *J Neurosci* **19**, 7230–7237.

Segev I & London M (1999). A theoretical view of passive and active dendrites. In *Dendrites*, ed. Stuart, G, Spruston, N & Hausser, M., pp. 205–230. Oxford University Press, New York.

Sjostrom PJ, Turrigiano GG & Nelson SB (2003). Neocortical LTD via coincident activation of presynaptic NMDA and cannabinoid receptors. *Neuron* **39**, 641–654.

Soltesz I, Smetters DK & Mody I (1995). Tonic inhibition originates from synapses close to the soma. *Neuron* **14**, 1273–1283.

Somogyi P, Tamas G, Lujan R & Buhl EH (1998). Salient features of synaptic organisation in the cerebral cortex. *Brain Res Brain Res Rev* **26**, 113–135.

Steriade M (2000). Corticothalamic resonance, states of vigilance and mentation. *Neuroscience* **101**, 243–276.

Trettel J & Levine ES (2002). Cannabinoids depress inhibitory synaptic inputs received by layer 2/3 pyramidal neurons of the neocortex. *J Neurophysiol* **88**, 534–539.

Trettel J & Levine ES (2003). Endocannabinoids mediate rapid retrograde signaling at interneuron–pyramidal neuron synapses of the neocortex. *J Neurophysiol* **89**, 2334–2338.

Tsou K, Mackie K, Sanudo-Pena MC & Walker JM (1999). Cannabinoid CB1 receptors are localized primarily on cholecystokinin-containing GABAergic interneurons in the rat hippocampal formation. *Neuroscience* **93**, 969–975.

Williams SR & Stuart GJ (2003). Role of dendritic synapse location in the control of action potential output. *Trends Neurosci* **26**, 147–154.

Wilson RI, Kunos G & Nicoll RA (2001). Presynaptic specificity of endocannabinoid signaling in the hippocampus. *Neuron* **31**, 453–462.

Wilson RI & Nicoll RA (2001). Endogenous cannabinoids mediate retrograde signalling at hippocampal synapses. *Nature* **410**, 588–592.

Yoshida T, Hashimoto K, Zimmer A, Maejima T, Araishi K & Kano M (2002). The cannabinoid CB1 receptor mediates retrograde signals for depolarization-induced suppression of inhibition in cerebellar Purkinje cells. *J Neurosci* **22**, 1690–1697.

Zilberter Y (2000). Dendritic release of glutamate suppresses synaptic inhibition of pyramidal neurons in rat neocortex. *J Physiol* **528**, 489–496.

Acknowledgements

This work was supported by National Institutes of Health Grants DA 16791 and DA 07312.